Chloropicrin Emissions after Shank Injection: Two-Dimensional Analytical and Numerical Model Simulations of Different Source Methods and Field Measurements

D. Wang,* S. R. Yates, and S. Gao

Understanding the control mechanisms of fumigant movement in soil is a fundamental step for developing management strategies to reduce atmospheric emissions. Most soil fumigants including chloropicrin (CP) are applied by shank injection, and the application process often leaves vertical soil fractures that would potentially cause preferential fumigant movement and increased emissions. This potential transport pathway was evaluated by comparing cumulative emissions and soil air concentrations of CP from direct field measurements with those predicted using analytical and numerical models after assuming either point or rectangle sources for the injected CP. Results clearly showed that shank-injected CP, when treated as vertical rectangle sources, produced cumulative emission losses similar to the field measurements. Treating the shanked CP as point sources caused approximately 50% underprediction than the field measurements. The study also demonstrated that fumigant cumulative emissions can be predicted, with reasonable accuracy, using either analytical or numerical simulations.

Chloropicrin (trichloronitromethane, CP) is commonly used as a component of commercial soil fumigants to enhance efficacy against soil-borne plant pathogens. Due to its strong lacrimatory properties, CP is also used as a warning agent to prevent exposure to colorless and odorless compounds such as methyl bromide (MeBr). Because of the phaseout of MeBr in the United States and other industrialized countries, demands for CP and other chemical alternatives are on the rise, at least in the short term, before integrated pest control strategies can be developed and deployed in commercial farming operations. Extensive efforts have been made to test the effectiveness of CP against a broad spectrum of soil pests ranging from fungal pathogens (Chellemi et al., 1994; Gullino et al., 2002; Louws et al., 2004) to nematodes (McKenry et al., 1998; Noling et al., 2001; Desaeger et al., 2004), weeds (Fennimore et al., 2003; Gilreath and Santos, 2005; Hanson and Shrestha, 2006), and insects (Moldenke and Thies, 1996). Although CP is not considered an ozone-deleting substance, research by Carter et al. (1997) and others showed that in the troposphere, CP enhanced NO oxidation and the formation of ground-level ozone. Because of their volatile and reactive nature, nearly all soil fumigants, including CP, are classified as toxic air contaminants (CDPR, 2010) and are strictly regulated to minimize human exposure risks (USEPA, 2009) and total volatile organic compound (VOC) emissions (CDPR, 2009).

Field and laboratory experiments have also been conducted to evaluate techniques to reduce atmospheric emissions of CP after soil application (Gan et al., 2000; Wang et al., 2005; Gao and Trout, 2007; Gao et al., 2008). Although drip application of CP is becoming available, in most commercial soil fumigation operations, CP is coapplied with MeBr or 1,3-dichloropropene (1,3-D, also known as Telone) by shank injection. It has been recognized that applying soil fumigants using shank knives creates vertical soil fractures behind each shank pass, which could potentially cause preferential fumigant emissions (Yates et al., 1997). Soil fracturing is difficult to characterize in field experiments because there are no other commercial means of applying concentrated CP to compare with the shank method. Furthermore, immediately following passage of the shanks, a second tractor pulling a disc and ring roller is used to disrupt the shank traces and compact the soil. This application process would likely leave the shank fractures

J. Environ. Qual. 40:1443–1449 (2011)
doi:10.2134/jeq2010.0233
Published online 21 Oct. 2010.
Received 21 May 2010.
*Corresponding author (dong.wang@ars.usda.gov).

5585 Guilford Rd., Madison, WI 53711 USA

D. Wang and S. Gao, USDA–ARS, Water Management Research Unit, Parlier, CA 93648; S.R. Yates, USDA–ARS, U.S. Salinity Lab., Riverside, CA 92507. Assigned to Associate Editor Mingxin Guo.

Abbreviations: 1,3-D, 1,3-dichloropropene; CP, chloropicrin; HDPE, high-density polyethylene; VIF, virtually impermeable film.

intact for depths below approximately 10 cm from the soil surface. The intact shank fractures could cause the fumigant gases to move quickly or preferentially, within the fractures, from the point of injection (25- to 66-cm depth) to the bottom of the compacted surface layer. Gas diffusion and dispersion would continue to transport the fumigant gases upward within the surface layer, reaching the soil surface and lost to atmospheric emissions. Little information exists concerning shank traces and effects on fumigant transport. The direct effect of subsurface shank fractures on fumigant emissions could not be determined by simply measuring and comparing the emission or gas exit rates directly above a shank pass or between shank passes because diffusion in the surface layer would include both vertical and lateral gas movement.

Simulation models have long been recognized as valuable tools for estimating the environmental fate and transport of volatile pesticides, including atmospheric volatilization (Jury et al., 1983; Wagenet et al., 1989). Atmospheric emissions of 1,3-D were simulated with a numerical pesticide model, LEACHM, using both gas diffusion and convective gas transport (Chen et al., 1995). In a different modeling study, the USEPA-certified one-dimensional numerical pesticide model, PRZM-3 (Carsel et al., 1995), was used to simulate 1,3-D emissions (Cryer et al., 2003). A two-dimensional finite element model, CHAIN_2D (Simunek and van Genuchten, 1994), was also parameterized to predict 1,3-D emissions (Wang et al., 2000; Cryer and van Wesenbeeck, 2010), with the latter empirically accounting for the shank trace as disturbed soil whose porosity had been altered above the surrounding undisturbed soil. This two-dimensional numerical model is capable of simultaneously solving the water, heat, and solute transport equations in the soil. More recently, analytical solutions were developed for predicting fumigant emissions under different surface boundary and initial conditions by simulating the shanks as either point or rectangle sources (Yates, 2009). Analytical solutions are useful because in some cases, simple algebraic expressions can be derived for computing fumigant emissions, whereas numeric simulations rely on iterative computational procedures that may be slow to run and sometimes subject to numerical errors and stability issues.

The objective of this study was to evaluate transport and volatilization mechanisms of shank-injected CP by comparing analytical and numerical model predictions under different surface boundary and initial conditions (point and rectangle sources) with field measurements. This research was motivated in part by a presentation for the Managing Agricultural Emissions Symposium at the 2009 American Chemical Society Annual Meeting and subsequent discussions of lack of understanding on the role of shank fractures in fumigant emissions.

Materials and Methods

Field Emission and Soil Property Measurements

The fumigation experiment used for model comparison was conducted in 2005 in the San Joaquin Valley of California (Gao et al., 2008), a major agricultural region with significant land acreage fumigated each year. The soil is a Hanford sandy loam (coarse-loamy, mixed, superactive, nonacid, thermic Typic Xerorthents). Telone C35 (61% 1,3-D and 35% CP a.i.) was applied at 746 kg ha^{-1} (or 261 kg ha^{-1} CP) to a 45-cm depth (18 inch) from the surface in a commercial orchard replant. Immediately after fumigant injection, soil surface was disced and compacted with a ring roller. Three surface treatments in the experiment, including bare soil, soil covered with a high-density polyethylene (HDPE, Tyco Plastics, Princeton, NJ) film, and soil covered with a virtually impermeable film (VIF, Bromostop, Bruno Rimini Corp., London, UK), were used for model comparisons. Fumigant emissions were measured using flux chambers and soil air concentrations measured with stainless steel gas probes (Gao et al., 2008). During the experiment, the soil water content was 0.02 cm^3 cm^{-3} near the surface and 0.10 cm^3 cm^{-3} at deeper depths. Average daily maximum air temperature was 20°C, and minimum ambient air temperature ranged from 3 to 12°C.

To determine soil hydraulic parameters for model simulation, soil core samples were collected from three field sites located within 1 km of the 2005 fumigation field. Soils from these sites belong to the same soil series as in the fumigated field. At each site, an open pit was excavated to a maximum depth of 2.25 m or to the depth of a hard pan. Replicated cores were collected from each pit at 10- to 30-cm increments. A constant head permeameter apparatus, modified from Klute and Dirksen (1986), was used to measure saturated hydraulic conductivity of these soil cores. A selected subset of the soil samples were tested at the University of California ANR Analytical Laboratory at Davis, CA, for chemical and water retention analysis. Water retention parameters (curves) were determined by first measuring soil water content at 10, 30, 100, and 1500 kPa and then fitting the data to the retention function of van Genuchten (1980). The soil properties showed a strong layering effect at approximately 20-cm depth. Therefore, the measured hydraulic conductivity and water retention data were averaged into two groups representing the 0- to 20-cm layer (thereafter termed material 1 or M1) and the layer below 20 cm (termed M2 thereafter) (Table 1).

Model Description and Parameterization

Similar to water evaporation, fumigant emission from the soil surface to the atmosphere is a boundary process that occurs in the vapor or gaseous phase. Because in most cases, a fumigant chemical is applied in soil below the surface, the rate of emission is described by a subsurface continuity equation, i.e., the total flux (liquid and gas by diffusion and convection) from below and moving toward the soil surface equals the flux leaving the soil surface and entering the atmosphere:

$$F = -D_{\mathrm{T}}\frac{\partial \mathrm{C}}{\partial z} + qC = -h\left(C_{\mathrm{g}} - C_{\mathrm{atm}}\right) \qquad [1]$$

where F is emission flux density (g cm^{-2} d^{-1}), D_{T} is total (gas and liquid) effective diffusion coefficient (cm^2 d^{-1}), C is fumigant concentration (g cm^{-3}), z is depth (cm), q is convective water flux (cm d^{-1}), h is mass transfer coefficient (cm d^{-1}), and C_{g} and C_{atm} are fumigant gas concentrations at and above the soil surface (g cm^{-3}), respectively.

At the soil–air interface, a thin stagnant air layer is often assumed, and fumigant passes through this layer by gas diffusion. For bare soil surfaces, the thickness of this thin layer is commonly assumed to be 5 mm (Jury et al., 1983). The mass transfer coefficient, h (Eq. [1]), can be calculated as the rate of gas diffusion in

pure air for a given chemical (CP in this case, 6672 $cm^2\ d^{-1}$) over the thickness of this layer. For soil surfaces covered with a layer of plastic film, the permeability of the film becomes the controlling factor, and the mass transfer coefficient, h, can be measured using laboratory procedures. To compare with the field experiment, the mass transfer coefficient (h) for CP was found to be 48 cm d^{-1} for HDPE and 9.6 cm d^{-1} for VIF (Papiernik and Yates, 2002). Papiernik et al. (2010) provides a compilation of mass transfer coefficients for CP for a variety of films.

The two-dimensional convective–dispersive equation for describing fumigant movement in soil can be written as follows (Simunek and van Genuchten, 1994):

$$\frac{\partial \theta C_L}{\partial t} + \frac{\partial \rho C_S}{\partial t} + \frac{\partial a_s C_g}{\partial t} = \frac{\partial}{\partial x_i}\left(\theta D_{ij}^w \frac{\partial C_L}{\partial x_j}\right) + \frac{\partial}{\partial x_i}\left(a_s D_{ij}^g \frac{\partial C_g}{\partial x_j}\right) - \frac{\partial q C_L}{\partial t} - \mu_w \theta C_L - \mu_s \rho C_s - S_r C_r \quad [2]$$

where C_L, C_S, and C_g are fumigant concentrations for the liquid, solid, and gaseous phases, respectively; μ_w and μ_s are first-order rate constants for fumigant in the liquid and solid phases, respectively; θ is the volumetric water content, ρ is the soil bulk density, a_s is the soil air content, S_r is the sink term in the water flow, C_r is the fumigant concentration in the sink term, D_{ij}^w is the dispersion coefficient tensor for the liquid phase, and D_{ij}^g is the diffusion coefficient tensor for the gas phase; t is time, x is distance, and indices i and j represent the horizontal and vertical directions, respectively. Degradation of CP in soil has been found to follow the first-order kinetics, and the half-life of CP is relatively short, ranging from 0.2 to 6.3 d (Dungan and Yates, 2003; Zhang et al., 2005; Qin et al., 2009). For model comparison with the field experiment, an average half-life of 3 d was used for both liquid and solid phases. The dimensionless Henry's law constant (K_h) is used to describe an instantaneous equilibrium between liquid and gas phase concentrations. In addition, values of μ_w, μ_s, K_h, and D_{ij}^g are temperature dependent and their dependency on temperature can be estimated using the Arrhenius equation:

$$p = p^{Tr} \exp\left(\frac{T - T_r}{RTT_r} E_a^p\right) \quad [3]$$

where p represents the parameters μ_w, μ_s, K_h, or D_{ij}^g, respectively, p^{Tr} is the value of p at a reference temperature T_r (20°C or 293 K), T is soil temperature (K), R is universal gas constant (8.314 J mol^{-1} K^{-1}), and E_a^p is activation energy (J mol^{-1}) for each of these parameters.

Shank-injected fumigants such as CP in soil can be considered as an instantaneous point or rectangle source in the two-dimensional simulation domain. For a point source, it can be described as

$$C_{L,g}(x, z, 0) = C_o\, \delta(x_i, z_i) \quad [4a]$$

$$C_{L,g}(x, z, 0) = 0 \text{ (elsewhere)} \quad [4b]$$

where C_o is the initial concentration of the fumigant (g cm^{-3}), δ is a delta function, and x_i and z_i describe the coordinate (cm) for fumigant injection (x_i = half the distance between shanks; z_i = 45 cm for the field experiment). For a rectangle source, it can be described as

$$C_{L,g}(x, z, 0) = C_o\, u(x_i - x_j)\, u(z_m - z_n) \quad [5]$$

where $x_i - x_j$ is the width of the rectangle (or width of the soil fracture created by a shank knife, assuming 3 cm for the field experiment), u is a unit step function with the property that $u(\zeta_i - \zeta_j) = 1$ when $\zeta_i \le \zeta \le \zeta_j$, and $z_m - z_n$ is the height of the rectangle (or the length of remaining intact soil fracture after

Table 1. Model parameters and values used in the analytical and numerical simulations.

Soil parameters	Analytical†	Numerical‡		
		M1	M2	M3
Initial soil water content ($cm^3\ cm^{-3}$)	0.06	0.02	0.11	0.01
Soil bulk density (g cm^{-3})	1.55	1.45	1.65	0.25
Residual soil water content ($cm^3\ cm^{-3}$)	NA	0.0200	0.0325	0.0100
Saturation soil water content ($cm^3\ cm^{-3}$)	0.4150	0.4528	0.3614	0.9000
Parameter α (cm^{-1})	NA	0.1680	0.0106	0.5000
Parameter n (-)	NA	2.0448	1.8554	5.0000
Soil hydraulic conductivity (cm d^{-1})	NA	1579	55	15,790
Soil sorption coefficient for CP ($cm^3\ g^{-1}$)	0.62	0.30	0.73	0.073
Parameters for both analytical and numerical simulations§				
Depth of injection (cm)	45			
Henry's law constant (–)	0.103			
First-order degradation coefficient (d^{-1})	0.231			
Mass transfer coefficient, bare soil (cm d^{-1})	13,344			
Mass transfer coefficient, HDPE (cm d^{-1})	48			
Mass transfer coefficient, VIF (cm d^{-1})	9.6			

† NA = not applicable because water flow is not simulated in the analytical solution and therefore no need for the water retention parameters or hydraulic conductivity.

‡ M1 represents material one or layer one for the 0- to 20-cm depth; M2 is material two or layer two for soils >20 cm; M3 represents material in shank trace, a rectangle covering 10- to 45-cm depth by 3-cm wide on a two-dimensional cross section. M3 disappears when injection treated as a point source.

§ HDPE, high-density polyethylene film; VIF, virtually impermeable film.

discing and roller packing, approximately 10 to 45 cm for the field experiment). The 45-cm (18-inch) injection depth is typically used for orchard replant soil fumigation.

To enhance fumigant distribution to deeper depths, a different shank design, termed *Bussing shank* (McKenry et al., 2003), extends the injection depth to 66 cm (26 inch) with two fumigant orifices at 45- and 66-cm depths, respectively. For annual crops, soil fumigants are usually placed at a shallower depth (nominally 10 inches or 25 cm). To further compare the point and rectangle source effect, these three injection methods or depths are compared for modeling assessment on CP emissions under bare soil conditions. A schematic diagram was drawn to show the shank layout as either point or rectangle sources (Fig. 1).

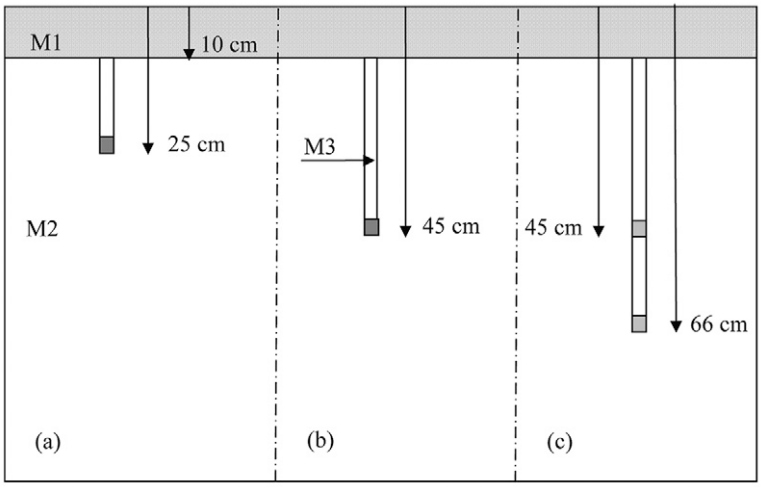

Fig. 1. Schematic diagram of shallow (a) 25-cm depth, deep (b) 45-cm depth, and Bussing (c) 45- and 66-cm depth for shank injection and rectangular shank fractures (M3, 3 cm in width) created during fumigant injection. Shaded area (M1) depicts compacted surface soil following disking and ring roller, and M2 represents undisturbed soil.

The numerical code CHAIN_2D (Simunek and van Genuchten, 1994) was used to predict CP emissions. To facilitate numerical simulations, rectangle sources were assumed to possess a dimension of 3 cm in width, a nominal thickness for the shank knives, and 15, 35, or 56 cm in length for the shallow, deep, and Bussing shank injection, respectively. Field observations showed that oftentimes the shank fracture was partially filled with very loose soil particles that probably fell in when discing the surface soil. There was no practical method of directly measuring the transport properties of the shank fractures. Therefore, material in the shank facture or the rectangle source was assigned a set of hydraulic parameters with extremely low retention capacity, and the material was termed M3. A comparison of water retention with the two soil layers (M1 and M2) is shown in Fig. 2. Water flow and heat transfer were also simulated, at the same time, to capture potential convective CP transport with water and temperature effect on CP movement in soil and emission into the atmosphere. Heat conduction in the soil was computed using the average surface air temperature and soil thermal properties for a sandy loam. A simulated 24-h soil temperature profile is shown to illustrate the soil temperature responses to the diurnal air temperature fluctuation (Fig. 3). Analytical solutions of Eq. [2] by Yates (2009) were used to predict CP emissions only for the 45-cm injection scenario by treating the fumigant as either a point or a rectangle source. Model parameters were based on reported values from Gao et al. (2008) and typical CP properties reported in the literature (Table 1). Soil water content and temperature were held as constants in the analytical solutions.

Results and Discussion

Predicted cumulative CP emissions were comparable to the measured values when rectangle sources were used in the model simulations (Table 2). Much lower emissions, compared to the field measurements, were predicted when shank injected CP were treated as point sources. This result was consistent for all three soil surface conditions (bare soil, HDPE, or VIF). For example, cumulative CP emission from the bare soil was approximately 30% of the applied chemical predicted by the rectangle source method, but the emissions reduced to about 14% when point sources were used in model predictions (Table 2). Therefore, it is apparent that shank fractures played a significant role in distributing CP and facilitating emission losses, at least for this particular experimental scenario.

Based on the cumulative emission data, it is also apparent that emission predictions compared well between the analytical solutions from Yates (2009) and numeric simulations using

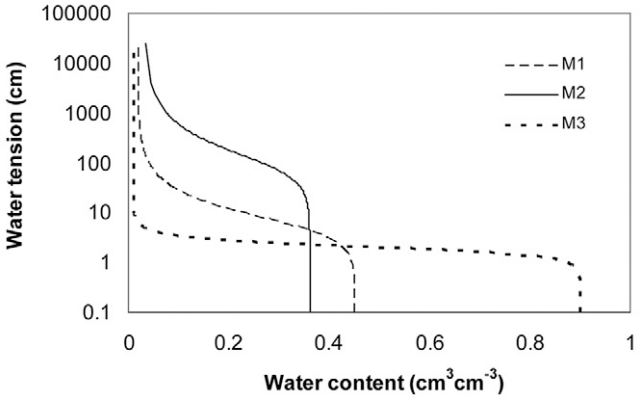

Fig. 2. Soil water retention curves used for numerical simulations. M1 is for 0- to 20-cm soil depth, M2 for more than 20-cm depth, M3 for the shank trace.

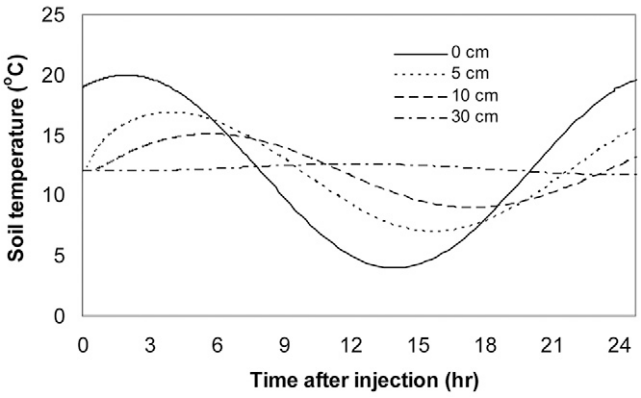

Fig. 3. Soil temperature variations predicted with the numerical model. Temperature-dependent Henry's constant, diffusion coefficient, and degradation rate were used in the numerical simulations.

Table 2. Comparison of predicted and measured cumulative chloropicrin emissions.

Soil surface†	Model setup	Cumulative emission		
		Analytical	Numerical	Measured
		%		
Bare soil	Point source	13.6	14.7	
	Rectangle source	32.5	29.1	30.0
HDPE	Point source	6.4	6.2	
	Rectangle source	15.4	13.1	17.0
VIF	Point source	2.1	1.8	
	Rectangle source	5.0	3.9	8.0

† HDPE, high-density polyethylene film; VIF, virtually impermeable film.

the Chain_2D codes (Simunek and van Genuchten, 1994), with the same assumed source. The analytical solutions were previously validated against a one-dimensional numeric model (Hydrus-1D) but not against two-dimensional applications. Compared to the two-dimensional numerical model, the analytical solutions worked quite well in predicting cumulative CP emissions for both the point and rectangle sources, even though water flow and temperature variations were not included. Water flow did not affect CP emission in this situation because the soil was rather dry at moisture 4% of the field capacity for M1 and 28% for M2 (Gao et al., 2008; Table 1), so there was minimal water movement. It is unlikely that the analytical model prediction method would perform well for drip fumigant applications or when irrigation is used to seal the soil surface as the effects of water flow would be important. Soil temperature also did not impact CP cumulative emissions because the analytical modeling used the average temperature of the diurnal maximum and minimum temperatures as used in the numeric model.

When the soil was covered with HDPE or VIF, CP concentrations at the soil surface were much higher than that when the soil was not covered (Table 3). At 156 h after injection, predicted concentrations were 619 ng cm^{-3} under HDPE and 968 ng cm^{-3} under VIF using the rectangle source method. This is attributed to the reduced emission losses when soil is covered with tarp and therefore significant amount of CP remained in the soil and was trapped underneath the tarp. The presence of surface tarps has the potential to lead to large emission peaks at tarp removal, which could pose a worker exposure risk. For these simulations, the presence of a VIF or HDPE increases potential exposure concentrations compared to bare soil. Modeling in this case can help estimate the duration that may be needed to keep the tarp in place until degradation has reduced the concentrations to acceptable levels. Modeling may also be used to evaluate techniques for accelerating fumigant degradation, such as surface amendments of highly reactive materials with the fumigants, so as to reduce the tarp cover time.

Table 3. Simulated chloropicrin concentrations at the soil surface or under the tarp directly above an injection shank pass at various elapsed times after fumigant application.

Soil surface†	Model setup	Chloropicrin concentration		
		12 h	36 h	156 h
		ng cm^{-3}		
Bare soil	Point source	0.02	2.6	2.5
	Rectangle source	11.4	12.9	4.0
HDPE	Point source	0.54	123	363
	Rectangle source	443	899	619
VIF	Point source	0.57	141	548
	Rectangle source	495	1110	968

† HDPE, high-density polyethylene film; VIF, virtually impermeable film.

The effect of treating the shank injection as either a rectangle source or point source was also depicted by CP gas distributions in the soil (Fig. 4). At 12 h after injection, the point

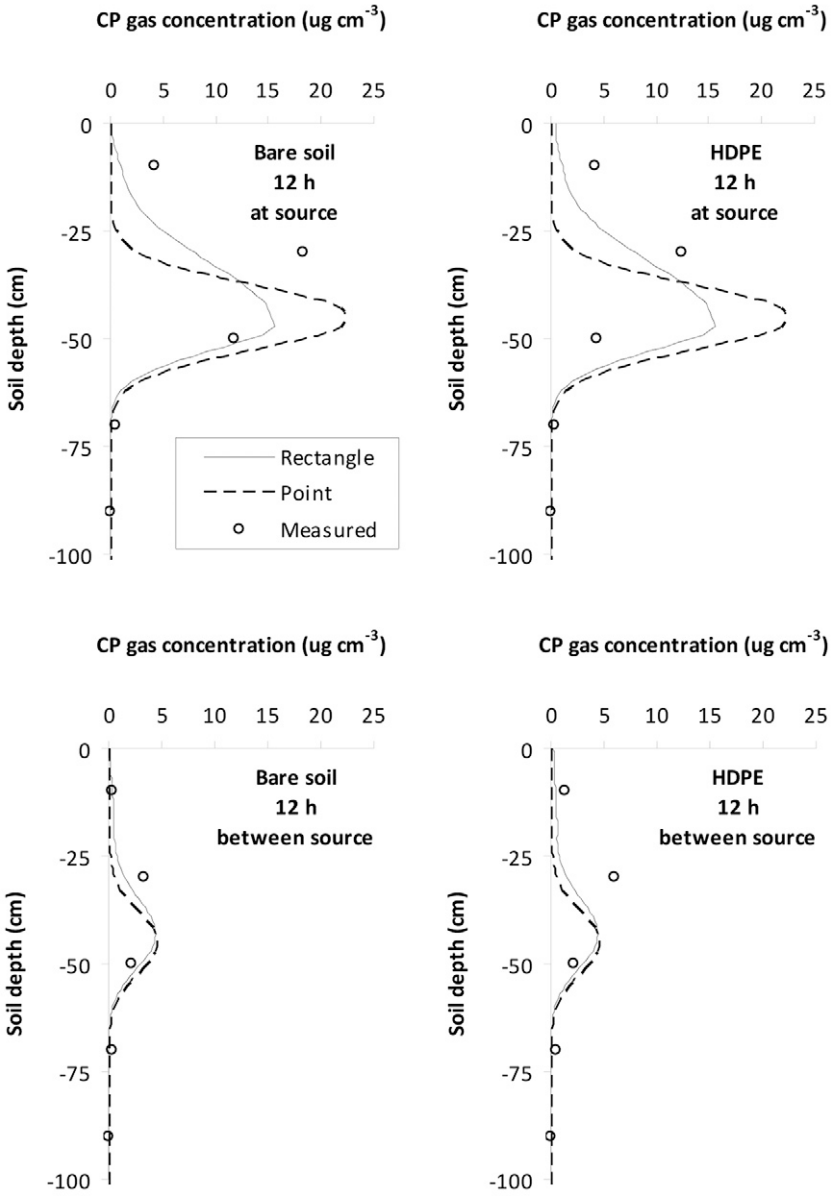

Fig. 4. Simulated chloropicrin (CP) concentrations in soil air 12 h after injection directly below a shank pass under bare soil or high-density polyethylene (HDPE) surface conditions and assuming the fumigant as either a rectangle (10- to 45-cm depth) or a point source at the 45-cm depth.

source assumption showed a relatively less dispersed CP peak than simulating a rectangle source where higher CP gas concentrations were found in the 0- to 35-cm depth under either bare soil or HDPE tarp cover. This effect was found both directly below a shank pass (or at source location) and halfway between two shank passes (or at the between source location). Based on Eq. [1], higher concentrations near the soil surface would create larger concentration gradients toward the soil surface, hence higher emissions. Measured CP gas concentrations appeared to match better with predictions using the rectangle source than the point source for both the at-source and between-source locations. The concentrations of CP under VIF were not included in the comparison because of missing data in measured CP concentrations.

Because of increased path length (to the soil surface) and resident time in the soil, it is conceivable that injecting fumigants to a deeper depth would reduce total and peak emissions and delay the occurrence of peak emissions. However, when shank-injected fumigants function as a rectangle source, with the depth of injection as the bottom and the disrupted surface soil as the top boundary of this imaginary narrow vertical rectangle, the effect of deeper injection on reducing total and peak emissions and delaying the occurrence of peak emissions could be less effective. This is exactly what was predicted with the model simulations when increasing the CP application depth from 25 cm to 45 and 66 cm using either the rectangle source or point source method as the model initial conditions (Fig. 5). Furthermore, the effect of rectangle source on CP emissions becomes more important when injection depth was at deeper depths. Comparing the rectangle source to the point source, cumulative CP emissions were 22% higher for 25 cm injection, and the difference increased to 49 and 41% for the 45-cm and Bussing (45 and 66 cm) injection methods, respectively (Table 4). The actual selection of injection depth is usually determined by crop type, for example, shallower for annual crops such as strawberries and tomatoes and deeper for perennials such as vines and trees. The modeling results indicate that when deeper shanks are used, it is more important to disrupt and minimize the shank source effect so fumigants would not move quickly to the soil surface. The effect has been considered in the design of the Bussing shank where one or two small metal plates were welded 15 cm above the 45-cm orifice for the sole purpose of disrupting the shank fractures (Hanson et al., 2007). However, after disrupting the fracture, if the fracture contains loose soil material, the transport of fumigant may be more rapid than the undisturbed soil region and may still lead to higher emissions. Clearly, more research is needed to improve application of soil fumigants, reduce emission losses,) and increase understanding of transport in typical production systems.

Conclusions

By comparing with direct field emission measurements, the modeling study clearly showed that shank-injected soil fumigants such as CP behave more like a vertical rectangle source than a point source. This is attributed to the creation and persistence of soil fractures and/or disturbed soil generated by the physical passage of shank knives in the soil and slight compaction when the metal knives were pulled across the field. Numerical results also showed that the effect of rectangle source on CP emissions was more pronounced for deep injections than shallow injections. Compared to "true" point sources, the effect of rectangle sources on fumigant emissions was also exhibited as increased total and peak emissions and accelerated occurrence of peak emissions. The modeling study also demonstrated and validated the accuracy of the analytical solutions for predicting cumulative fumigant emissions.

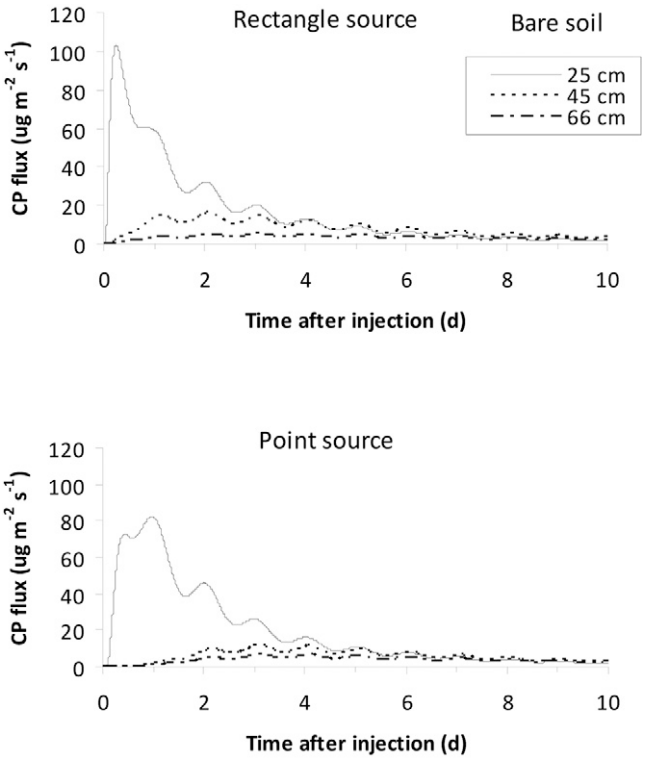

Fig. 5. Simulated chloropicrin (CP) emission flux from bare soil when treating the injection as a rectangle or point source at shallow (25-cm), deep (45-cm), and Bussing (45- and 66-cm) applications.

Table 4. Comparison of simulated cumulative chloropicrin bare soil emissions (%) when treating the injection as a point or rectangle source at 25-, 45-, and both 45- and 66-cm depth applications.

Model setup	Injection depth		
	25	45	45+66
		cm	
Point source	51.6	14.7	8.9
Rectangle source	65.8	29.1	15.1

Acknowledgments

We thank Prof. Luke Wang of California State University Fresno for lending us the constant head permeameter for measuring hydraulic conductivity and Jim Gartung and Matthew Gonzales for assisting the measurements of the soil parameters.

References

Carsel, R.F., J.C. Imhoff, P.R. Hummel, J.M. Cheplick, and A.S. Donigan, Jr. 1995. PRZM-3, A model for predicting pesticide and nitrogen fate in the crop root and unsaturated soil zones: Users manual for release 3.0. National Exposure Research Laboratory, Office of Research and Development, USEPA, Athens, GA.

Carter, W.P.L., D.M. Luo, and I.L. Malkina. 1997. Investigation of the atmospheric reactions of chloropicrin. Atmos. Environ. 31:1425–1439.

California Department of Pesticide Regulation (CDPR). 2009. Reducing VOC emissions from field fumigants. Cal EPA, Sacramento, CA. Available at http://www.cdpr.ca.gov/docs/emon/vocs/vocproj/reg_fumigant.htm (verified 12 Oct. 2010).

California Department of Pesticide Regulation (CDPR). 2010. Toxic air contaminant program: Final toxic air contaminant (TAC) evaluation reports and determinations—Chloropicrin. Available at http://www.cdpr.ca.gov/docs/emon/pubs/tac/finaleval/chloropicrin.htm (verified 12 Oct. 2010).

Chellemi, D.O., S.M. Olson, and D.J. Mitchell. 1994. Effects of soil solarization and fumigation on survival of soilborne pathogens of tomato in northern Florida. Plant Dis. 78:1167–1172.

Chen, C., R.E. Green, D.M. Thomas, and J.A. Knuteson. 1995. Modeling 1,3-dichloropropene fumigant volatilization with vapor-phase advection in the soil profile. Environ. Sci. Technol. 29:1816–1821.

Cryer, S.A., and I.J. van Wesenbeeck. 2010. Estimating field volatility of soil fumigants using CHAIN_2D: Mitigation methods and comparison against chloropicrin and 1,3-dichloropropene field observations. Environ. Model. Assess. 15:309–318.

Cryer, S.A., I.J. van Wesenbeeck, and J.A. Knuteson. 2003. Predicting regional emissions and near-field air concentrations of soil fumigants using modest numerical algorithms: A case study using 1,3-dichloropropene. J. Agric. Food Chem. 51:3401–3409.

Desaeger, J.A.J., J.E. Eger, A.S. Csinos, J.P. Gilreath, S.M. Olson, and T.M. Webster. 2004. Movement and biological activity of drip-applied 1,3-dichloropropene and chloropicrin in raised mulched beds in the southeastern USA. Pest Manag. Sci. 60:1220–1230.

Dungan, R.S., and S.R. Yates. 2003. Degradation of fumigant pesticides: 1,3-dichloropropene, methyl isothiocyanate, chloropicrin, and methyl bromide. Vadose Zone J. 2:279–286.

Fennimore, S.A., M.J. Haar, and H.A. Ajwa. 2003. Weed control in strawberry provided by shank- and drip-applied methyl bromide alternative fumigants. HortScience 38:55–61.

Gan, J., S.R. Yates, F.F. Earnst, and W.A. Jury. 2000. Degradation and volatilization of the fumigant chloropicrin after soil treatment. J. Environ. Qual. 29:1391–1397.

Gao, S., and T.J. Trout. 2007. Surface seals reduce 1,3-dichloropropene and chloropicrin emissions in field tests. J. Environ. Qual. 36:110–119.

Gao, S., T.J. Trout, and S. Schneider. 2008. Evaluation of fumigation and surface seal methods on fumigant emissions in an orchard replant field. J. Environ. Qual. 37:369–377.

Gilreath, J.P., and B.M. Santos. 2005. Efficacy of 1,3-dichloropropene plus chloropicrin in combination with herbicides on purple nutsedge (*Cyperus rotundus*) control in tomato. Weed Technol. 19:137–140.

Gullino, M.L., A. Minuto, G. Gilardi, A. Garibaldi, H. Ajwa, and T. Duafala. 2002. Efficacy of preplant soil fumigation with chloropicrin for tomato production in Italy. Crop Prot. 21:741–749.

Hanson, B.D., and A. Shrestha. 2006. Weed control with methyl bromide alternatives. CAB Rev. Perspect. Agric. Vet. Sci. Nutr. Nat. Resour. 63:1–13.

Hanson, B., S. Gao, M. McKenry, J. Gerik, D. Wang, K. Klonsky, D. Cox, B. Correiar, and S. Yates. 2007. Efficacy and 1,3-D emission with approved nursery stock certification treatments applied with two shank designs. p. 13(1–3). *In* Proc. Int. Res. Conf. Methyl Bromide Alternatives and Emission Reductions, San Diego, CA. 29 Oct.–1 Nov. 2007. Available at http://mbao.org/2007/Proceedings/mbrpro07.html (verified 12 Oct. 2010).

Jury, W.A., W.F. Spencer, and W.J. Farmer. 1983. Behavior assessment model for trace organics in soil: I. Model description. J. Environ. Qual. 12:558–564.

Klute, A., and C. Dirksen. 1986. Hydraulic conductivity and diffusivity: Laboratory methods. p. 687–732. *In* A. Klute (ed.) Methods of soil analysis. Part 1. Physical and mineralogical methods. 2nd ed., Madison, WI.

Louws, F.J., L.M. Ferguson, K. Ivors, J. Driver, K. Jennings, D. Milks, P.B. Shoemaker, and D.W. Monks. 2004. Efficacy of methyl bromide alternatives for Verticillium and weed management in tomatoes. p. 43(1–3). *In* Proc. Int. Res. Conf. Methyl Bromide Alternatives and Emission Reductions, Orlando, FL. 31 Oct.–3 Nov. 2004. Available at http://mbao.org/2004/Proceedings04/mbrpro04.html (verified 12 Oct. 2010).

McKenry, M.V., D. Buessing, and K. Williams. 2003. New chisel shanks enable improved fumigation of finer-textured soils. p. 36(1–3). *In* Proc. Int. Res. Conf. Methyl Bromide Alternatives and Emission Reductions, San Diego, CA. 3–6 Nov. 2003. Available at http://mbao.org/2003/mbrpro03.html (verified 12 Oct. 2010).

McKenry, M.V., B. Hutmacher, and T. Trout. 1998. Nematicidal value of eighteen preplant treatments one year after replanting susceptible and resistant peach rootstocks. p. 34(1–3). *In* Proc. Int. Res. Conf. Methyl Bromide Alternatives and Emission Reductions, Orlando, FL. 7–9 Dec. 1998. Available at http://mbao.org/mbrpro98.html (verified 12 Oct. 2010).

Moldenke, A.R., and W.G. Thies. 1996. Application of chloropicrin to control laminated root rot: Research design and seasonal dynamics of control populations of soil arthropods. Environ. Entomol. 25:925–932.

Noling, J.W., J.P. Gilreath, and E.R. Rosskopf. 2001. Alternatives to methyl bromide field research efforts for nematode control in Florida. p. 14(1–3). *In* Proc. Int. Res. Conf. Methyl Bromide Alternatives and Emission Reductions, San Diego, CA. 5–9 Nov. 2001. Available at http://mbao.org/2001proc/mbrpro01.html (verified 12 Oct. 2010).

Papiernik, S.K., and S.R. Yates. 2002. Effect of environmental conditions on the permeability of high density polyethylene film to fumigant vapors. Environ. Sci. Technol. 26:1833–1838.

Papiernik, S.K., S.R. Yates, and D.O. Chellemi. 2010. A standardized approach for estimating the permeability of plastic films to soil fumigants under various field and environmental conditions. J. Environ. Qual. 40:1375–1382. doi:10.2134/jeq2010.0118 (this issue).

Qin, R., S. Gao, H. Ajwa, B. Hanson, T. Trout, D. Wang, and M. Guo. 2009. Interactive effect of organic amendment and environmental factors on degradation of 1,3-dichloropropene and chloropicrin in soil. J. Agric. Food Chem. 57:9063–9070.

Simunek, J., and M.Th. van Genuchten. 1994. The CHAIN-2D code for simulating the two-dimensional movement of water, heat, and multiple solutes in variably-saturated porous media. Version 1.1. Research Rep. 136. U.S. Salinity Laboratory, USDA–ARS, Riverside, CA.

USEPA. 2009. Pesticides: Reregistration—Chloropicrin. USEPA, Washington, DC. Available at http://www.epa.gov/oppsrrd1/reregistration/chloropicrin/ (verified 11 May 2010).

van Genuchten, M.Th. 1980. A close-form solution for predicting the conductivity of unsaturated soils. Soil Sci. Soc. Am. J. 44:892–898.

Wagenet, R.J., J.L. Hutson, and J.W. Biggar. 1989. Simulating the fate of a volatile pesticide in unsaturated soil: A case study with DBCP. J. Environ. Qual. 18:78–84.

Wang, D., J. Juzwik, S.W. Fraedrich, K. Spokas, Y. Zhang, and W.C. Koskinen. 2005. Atmospheric emissions of methyl isothiocyanate and chloropicrin following soil fumigation and surface containment treatment in bare-root forest nurseries. Can. J. For. Res. 35:1202–1212.

Wang, D., J.A. Knuteson, and S.R. Yates. 2000. Two-dimensional model simulation of 1,3- dichloropropene volatilization and transport in a field soil. J. Environ. Qual. 29:639–644.

Yates, S.R. 2009. Analytical solution describing pesticide volatilization from soil affected by a change in surface condition. J. Environ. Qual. 38:259–267.

Yates, S.R., D. Wang, F.F. Ernst, and J. Gan. 1997. Methyl bromide emissions from agricultural fields: Bare-soil, deep injection. Environ. Sci. Technol. 31:1136–1143.

Zhang, Y., K. Spokas, and D. Wang. 2005. Degradation of methyl isothiocyanate and chloropicrin in forest nursery and agricultural soils. J. Environ. Qual. 34:1566–1572.